Self-Organized Dynamics on a Curved Growth Interface

S. Bottin-Rousseau[1,2] and A. Pocheau[1]

[1]*IRPHE, CNRS UMR 6594, Universités Aix-Marseille I & II, 49 rue Joliot-Curie, B.P. 146, Technopole de Château-Gombert, F-13384 Marseille Cedex 13, France*

[2]*Groupe de Physique des Solides, CNRS UMR 7588, Universités Denis Diderot et Pierre et Marie Curie, Tour 23, 2 Place Jussieu, F-75251 Paris Cedex 05, France*

(Received 15 December 2000; published 26 July 2001)

We experimentally address long-time dynamics of an artificially curved growth interface in directional solidification. Repetitive cell nucleations are found to appear in a disordered way, but to eventually organize themselves in a coherent way, for long times. This behavior is recovered by simulation of a nonlinear advection-diffusion model for phase dynamics. The existence of a periodic attractor is supported by the derivation of a Lyapunov functional for this model.

DOI: 10.1103/PhysRevLett.87.076101 PACS numbers: 81.10.Aj, 05.65.+b, 47.54.+r, 81.30.Fb

Far enough from equilibrium, physical or biological growth interfaces undergo various instability mechanisms that generate cellular distortions [1,2]. These shape modulations are of paramount importance for modeling effective features of interfaces such as their mean growth velocity or their net flux balance, as well as for determining the resulting properties of the surrounding media. For this reason, they have drawn a great deal of attention in various systems, both in linear and nonlinear regimes [3]. However, whereas most experimental configurations and models assume planar interfaces on large scales, those encountered in nature usually involve a slight curvature due to a large scale perturbation [4], a large scale instability [3,5], or a closed interface geometry [3,6,7]. This Letter is devoted to experimentally investigate whether weak curvature can generate specific phenomena that are important enough to modify the global behavior of growth interfaces. For this, attention will be focused on the canonical example of directional solidification.

Directional solidification [1,4,8] consists of pulling a liquid mixture in a thermal gradient so as to force it to solidify at a controlled velocity V. Above a certain critical velocity, V_c, a primary instability generates cellular distortions of the growth interface [1]. In thin samples, however, interfaces are usually planar on scales large compared to cell widths, so that cell dynamics satisfy an *average* left/right symmetry. In contrast, interfaces in thick samples usually display a large scale curvature, due to temperature modulations or to natural convection, for instance. In this case, left/right symmetry of the mean growth conditions is not maintained. In this sense, the objective of this study is to investigate the spatiotemporal implications of this symmetry breaking.

What makes this experiment distinct is that we *artificially* introduce a controlled interface curvature on a scale *large* compared to the cell scale. For this, solidification is studied in thin samples so as to avoid 3D disturbances and convection [8], but in a configuration where equilibrium interfaces are *bent*. In view of the large difference between the curvature radius ρ of the interfaces and the typical cell width $\lambda \ll \rho$, the induced modification seems weak, especially at the individual cell level. However, it will prove to dramatically change the spatiotemporal organization of the growth front by yielding spatial homogeneity, repetitive instabilities, and dynamical synchronization. A simple model of nonlinear advection diffusion for phase modulation will corroborate this finding. Interestingly, it shows diffusion yielding, as in the Turing mechanism [9], a surprising pattern organization.

The experimental setup simply generates large scale curvature by bending isothermal lines. This is obtained by altering the boundary conditions for the thermal field from straight parallel lines [10] to broken lines delimiting a V-shaped channel (Fig. 1). Smoothing out of the temperature field away from the boundaries then makes isothermal lines bend on the scale of the channel. Although this configuration produces noticeable variations of chemical or thermal gradient fields on the whole setup, relevant control parameters will nevertheless be fairly constant on the small domain studied hereafter.

The samples are made by sandwiching a 75 μm thick layer of nominally pure succinonitrile, a transparent material, between two parallel glass plates, 45×150 mm^2 wide. (NMR) experiments show a *single* chemical bond different from those of succinonitrile [11]. It corresponds

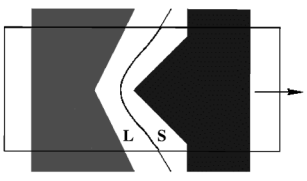

FIG. 1. Sketch of the V-shaped oven including the melting isothermal line. Rectangular sample, 45×150 mm^2 wide, is pushed from the hot side to the cold side, i.e., from the liquid phase (L) to the solid phase (S). The interface part studied, 2.2 mm wide, extends on one-twentieth of the sample width. It is centered on the symmetry axis of the setup.

to a *single* noticeable impurity: ethylene. Its solutal diffusivity in the liquid phase $D \approx 1.35 \times 10^{-5} \pm 0.05 \times 10^{-5}\ \mathrm{cm^2\,s^{-1}}$, partition coefficient $k = 0.3 \pm 0.05$, and impurity concentration $c_\infty = 2.9\ \mathrm{mol\,\%}$ have been deduced from measurements of the critical velocity V_c, the melting temperature T_L, and the solidification temperature T_S [11], given the thermodynamic data of pure succinonitrile. Nonintrusive observation of the solidification front is achieved by a shadowgraph technique. The channel gap is 7 mm at its tip and the temperature at the hot and cold boundaries is 10 and 100 °C, respectively. In the domain studied below, the temperature gradient decreases from $105\ \mathrm{K\,cm^{-1}}$ at the channel tip to $100\ \mathrm{K\,cm^{-1}}$ at the domain boundaries. The critical velocity at the channel tip, $V_c = 1.1 \pm 0.1\ \mu\mathrm{m\,s^{-1}}$, has been determined as the onset of front destabilization for waiting times as long as $16\tau_D$, where $\tau_D = D/V^2$ is the impurity diffusion time. In the sequel, the relevant scales will be the front curvature radius $\rho = 7$ mm and the cell width $\lambda \approx 80\ \mu$m.

The present study is restricted to a small domain around interface tip (width 2.2 mm, i.e., about $\rho/3$) and to the vicinity of its primary instability: $V_c < V < 2V_c$. At a fixed V, one then observes cells involving narrow grooves and showing a *constant* evolution (Fig. 2). They actually drift along the interface and widen until they reach a critical width λ_c at which they *split* into two cells of size $\lambda_c/2$ (Fig. 2b). Each new cell then resumes evolution by growing until splitting into a new couple of cells, etc. This stretch-induced tip splitting is reminiscent of that arising in radial fingering [7] and of the convective instabilities forced by a mean flow [12]. It gives rise to successive generations of cells with length bounded in between $[\lambda_c/2, \lambda_c]$ by an instability.

This basic behavior of the growth front directly results from the virtual tangential flow V_τ induced by the interface curvature in the reference frame of the growing interface. By "virtual," it is meant that the liquid mixture is actually at rest in the sample frame but appears to glide along the front in its own frame. This flow, which actually breaks the left/right symmetry on the front, is then responsible not only for cell drift but also for cell enlargement. In particular, denoting s the curvilinear abscissa taken from the tip and $\theta \approx s/\rho$ the angle between the interface normal and the pulling direction, one has $V_\tau = V \sin(\theta)$. The flow V_τ thus strictly vanishes at the tip ($\theta = 0$) and, at first approximation, grows linearly with curvilinear abscissa s: $V_\tau \approx Vs/\rho$. Accordingly, two interface points separated by a distance l undergo a tangential velocity difference $\delta V_\tau = Vl/\rho$, following which their distance increases exponentially with time: $l(t) = l(0)\exp(Vt/\rho)$. This generates an exponential *stretch* of the cells.

As soon as the interface is curved ($\rho < \infty$), its dynamics are thus sustained by relaxation oscillations of cell width in between $\lambda_c/2$ and λ_c. This may be easily exemplified on spatially homogeneous growth states, since stretch by tangential flow then stands as the *only* factor of cell dynamics. The time scale τ of cell width oscillations is then simply set by the pulling velocity and the curvature, $\lambda(t) = \lambda_c/2\exp(t/\tau)$ with $\tau = \rho/V$, so that the lifetime T_c of the cells reads $T_c = \tau \ln(2)$. On the other hand, for other states involving different cell widths, thin cells tend to expand at the expense of neighboring fat cells, thereby modifying the growth law of individual cells. However, the previous law nevertheless remains valid on *average* over a large portion of the interface, because the size reduction of one cell is compensated by the size extension of another. In particular, the number of cell nucleations observed over time t in an area of size L reads $N(t) = L/\lambda_c\ t/T_c = 1/\ln(2)\ L/\lambda_c\ Vt/\rho$. Quite good agreement with experiment is found in Fig. 3.

Beyond this average evolution, we now wish to focus our attention on the spatiotemporal organization of the growth interface by investigating whether cell nucleations occur in a disordered way or in a coherent way. For this, we made spatiotemporal diagrams of interface dynamics over about $8T_c$, i.e., 5 h (Fig. 4). These are obtained by plotting successive image cuts of the cellular interface by a fixed curve, its mean profile. Cuts are performed at a fixed frequency just below cell tips and placed one beside the other. Trajectories of cell grooves are detected as dark lines. Their drift clearly shows curvature-induced advection. Also, cell nucleations are detected by the occurrence of new grooves, i.e., new dark lines.

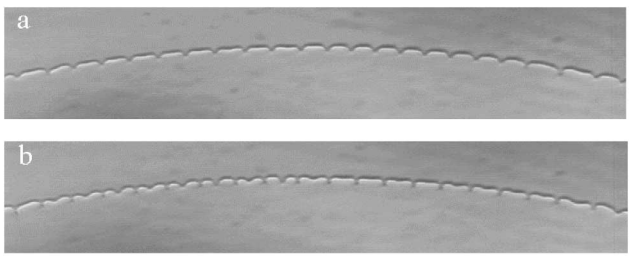

FIG. 2. Snapshots of the cellular solidification front. Image width is 2.2 mm and $V = 1.6\ \mu\mathrm{m\,s^{-1}}$. Solid phase is below the interface. (a) On the left side, large cells are displayed as a result of the stretch produced by the tangential flow driven by interface curvature. These cells are ready to split. (b) A few minutes later, these cells start to split.

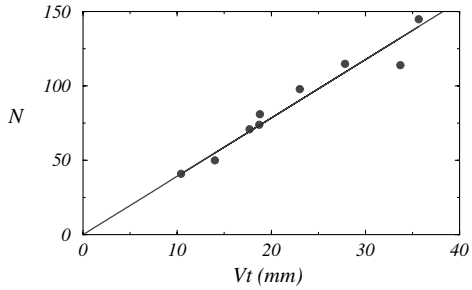

FIG. 3. The number of splits in a curved area of size $L = 19\lambda_c$ involving a curvature radius $\rho = 7$ mm. Both pulling velocity V and growth time t have been varied. The line corresponds to the expected relationship $N(t) = L/\lambda_c\ t/T_c = 1/\ln(2)\ L/\lambda_c\ Vt/\rho$.

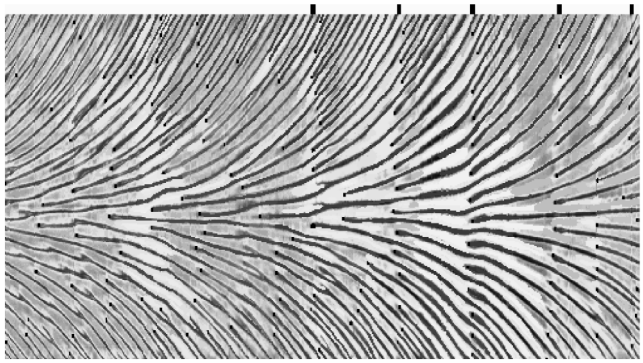

FIG. 4. Spatiotemporal diagram of the growth front for $V = 2.2\ \mu\mathrm{m\,s^{-1}}$. Width of the observed interface is 2.2 mm and observation time is 5 h. Curvilinear abscissa is vertical and time increases from left to right. Cell grooves appear as dark lines and cell splits are identified as new dark lines. Surprisingly, global regular events (marked in black at the top of the diagram) are seen in the asymptotic regime.

Figure 4 shows a typical spatiotemporal organization arising from the beginning of growth. Just after the onset of growth, cell nucleations appear on isolated cells or, at best, on groups of a few cells. In this sense, cell dynamics are disordered since there is no long-range spatial or temporal coherence. However, as time goes on, groups of quasisimultaneous nucleations include more and more cells. Finally, after a few lifetimes T_c, nucleations surprisingly appear as an *avalanche,* thereby giving rise to a sudden cascade of nucleations in the spatiotemporal diagram. The fact that successive nucleation cascades involve nearly the same shape and the same delay reveals that a *long-range periodic* dynamics has been reached.

When repeating growth in the same sample, a slight drift of characteristic variables occurs, owing to the mean lateral diffusion of impurity concentration induced by interface curvature. However, the important fact is that long-range periodic dynamics are always established after a long period of time, whatever the initial conditions.

The origin of the synchronization of nucleations may be sought in factors either common to all interfaces, e.g., cell interaction, or specific to curved ones, e.g., the slight variations of impurity concentration or of temperature gradient on the interface. However, by implementing a model of cellular phase dynamics, we show below that cell interaction is sufficient to recover this synchronization.

We introduce a phase variable $\varphi(s,t)$ labeling cell position and varying by 2π on a cell. Its dynamics result from the advection by a tangential flow V_τ and the interaction between neighboring cells. According to the usual procedure worked out in weakly distorted systems [3,13], we model neighbor interaction by a phase gradient expansion. Notice that, besides the resulting advection, curvature does not favor any direction or position along the interface, since both the thermal gradient and the concentration gradient remain everywhere normal to it. Therefore, only even phase derivatives are allowed to model cell interactions here. Moreover, as the phase dynamics are stable

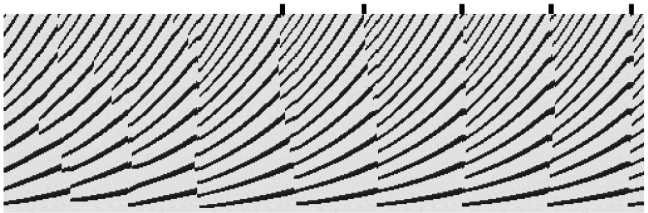

FIG. 5. Spatiotemporal diagrams derived from numerical simulation of (1). Only the left part of the front is shown on the same number of cells and over the same time as in Fig. 4. Initial conditions are inhomogeneous: $\partial q/\partial s \neq 0$. Notice the synchronization of nucleations in the asymptotic regime.

between nucleations, the first relevant expansion term, i.e., the second phase derivative $\partial^2\varphi/\partial s^2$, is sufficient to model phase interactions [13]. Relevant nonlinearities are taken into account by allowing the phase diffusion coefficient D to vary with wave number $q = \partial\varphi/\partial s \approx 2\pi/\lambda(t)$. Accounting for the cell advection by the flow $V_\tau = s/\tau$ by a total derivative of φ, one then obtains a nonlinear advection-diffusion equation for phase dynamics, reminiscent of the pattern formation modeling within a mean flow [12]:

$$\frac{\partial\varphi}{\partial t} + V_\tau \frac{\partial\varphi}{\partial s} = D(q)\frac{\partial^2\varphi}{\partial s^2}. \qquad (1)$$

Positive (respectively, negative) values of D mean relaxation (respectively, amplification) of spatial heterogeneity [3]. In particular, the vanishing of D corresponds to the onset of cell nucleation by Eckhaus instability, i.e., to $q_c = 2\pi/\lambda_c$ here. In its vicinity, higher order terms would be required to accurately model the phase evolution. However, at nucleation, the phase gradient expansion breaks down.

This model is "minimal" in the sense that it adds only phase advection to the phase dynamics of planar interfaces. However, we show below, both on numerical and theoretical grounds, that it succeeds in recovering repetitive cell nucleations and their synchronization.

To perform numerical simulation of phase dynamics for long periods of time, one must complete the model (1) to account for cell nucleations. We do it empirically by introducing an additional cell whenever the effective diffusion coefficient D vanishes. As this trick does not account for the real phase field brought about by cell nucleation, one might fear the occurrence of large cumulative errors. However, changing the fine structure of the additional phase field gave no qualitative implication on the long term. A nearly parabolic form of $D(q)$ vanishing at finite q has been taken [14], in agreement with the canonical expression of D for small amplitude stationary patterns [3]. This choice is not crucial however, since front behavior proves to be qualitatively independent of the detailed form of $D(q)$, provided that $D(q)$ is convex and vanishes at finite q. Simulations then show spatiotemporal diagrams that closely resemble the experimental ones (Fig. 5). In particular, coherence of cell nucleations is reached over few nucleation

sequences. Moreover, the fact that avalanches occur nearly simultaneously on all cells reveals that their wave number is almost the same. The growth front has then reached a spatially *homogeneous* state with *periodic* dynamics.

Attraction to regular dynamics may be shown by considering the functional:

$$\mathcal{F}(t) = \frac{1}{2}\int_0^L \left(\frac{\partial \tilde{q}}{\partial \tilde{s}}\right)^2 d\tilde{s}\,. \tag{2}$$

Here L is the length of a given interface part $\mathcal{P}$ at initial time $t = 0$, $\tilde{s} = \sigma(t)^{-1}s$, $\tilde{q} = (\partial\varphi/\partial\tilde{s})_t$, and $\sigma(t) = \exp(t/\tau)$ denotes the interface stretch factor at time t. Curvilinear abscissa $\tilde{s}$ corresponds to the interface coordinate once stretch is removed, i.e., in the frame of the stretched substrate. In particular, whereas advection stretches the interface, $s \to \sigma(t)s$, it leaves the Lagrangian coordinate $\tilde{s}$ unchanged: $\tilde{s} \to \tilde{s}$. Thus, integrating at time t over the interval $0 \le \tilde{s} \le L$ means integrating over the interface part which was initially located at $0 \le s \le L$. In this substrate frame $(\tilde{s}, t)$, the cell wave number reads $\tilde{q} = \sigma q$ and phase dynamics (1) satisfy a nonautonomous nonlinear diffusion equation:

$$\left.\frac{\partial\varphi}{\partial t}\right|_{\tilde{s}} = \sigma^{-2}(t) D \left.\frac{\partial^2\varphi}{\partial\tilde{s}^2}\right|_t . \tag{3}$$

Differentiating (3) with respect to Lagrangian coordinate $\tilde{s}$ and (2) with respect to time t and denoting $D' = dD/dq$, $D'' = d^2D/dq^2$, gives, by twice integrating by parts:

$$\frac{d\mathcal{F}}{dt} = \left[\frac{\partial q}{\partial\tilde{s}}\left\{D\frac{\partial^2 q}{\partial\tilde{s}^2} + \frac{2}{3}D'\left(\frac{\partial q}{\partial\tilde{s}}\right)^2\right\}\right]_0^L - \int_0^L \left[D\left(\frac{\partial^2 q}{\partial\tilde{s}^2}\right)^2 - \frac{D''}{3}\left(\frac{\partial q}{\partial\tilde{s}}\right)^4\right] d\tilde{s}\,. \tag{4}$$

Relation (4) enables us to follow the evolution of a compact wave number distortion surrounded by uniform cell width domains. Consider an interface part $\mathcal{P}$ englobing this distortion domain. As the wave number gradient $\partial q/\partial\tilde{s}$ vanishes at its end points $\tilde{s} = 0, L$, the boundary terms in relation (4) vanish. This persists at least until the wave number distortion reaches the boundaries of $\mathcal{P}$. Meanwhile, the functional variation $d\mathcal{F}/dt$ is *negative* since D is positive within the cell stability band and D'' is negative [14]. This means that $\mathcal{F}$ is a *Lyapunov functional* of the front evolution.

As the functional $\mathcal{F}$ only involves Lagrangian variables $(\tilde{s}, \tilde{q}, L)$, its decrease with time is not due to the interface stretch. Instead, it refers to the constant evolution of the interface towards better spatial uniformity in between nucleations. As spatial uniformity yields periodicity here, this supports the fact that the growth interface attains self-organization for large times.

We have demonstrated experimentally that large scale curvature of a growth interface yields an asymptotically organized regime involving spatial homogeneity and periodic dynamics. The mechanism of this organization is in two stages: first, dynamics is triggered by instability; then, it succeeds in reaching periodic states. From numerical simulation and derivation of a Lyapunov functional, we have shown that these behaviors can be recovered within the simplest model for phase dynamics: advection of the cell phases by the tangential flow supplemented by nonlinear diffusive interaction between them.

As the ingredients of this model are common to some growth interfaces, their consequences could extend to systems other than those studied here. For instance, in eutectic colonies, a large scale instability naturally gives rise to an interface curvature [5]. Moreover, the interface stretch responsible for repetitive cell nucleations could equally be produced in other systems by other means than the present virtual flow V_τ: real convective flows in 3D solidification [4], radial expansion of a swarm ring in bacteria colonies [6], or radial expansion of a viscous interface in radial fingering [7]. As found here, diffusion could then be sufficient to solely induce the synchronization of nucleations. Interestingly, this reveals its surprising ability in organizing systems on a long range, as in the formation of Turing patterns [9]. On a more general note, the present experiment and its analysis show that slightly distorting growth interfaces on a scale large compared to the width of their cells can represent a simple method for dynamically regulating growth patterns.

We thank M. Georgelin and E. Villermaux for stimulating discussions and J. Minelli for technical assistance. S. B.-R. thanks the CNES for financial support.

[1] W. W. Mullins and R. F. Sekerka, J. Appl. Phys. **35**, 444 (1964).
[2] H. G. E. Hentschel and A. Fine, Phys. Rev. Lett. **73**, 3592 (1994).
[3] M. C. Cross and P. C. Hohenberg, Rev. Mod. Phys. **65**, 851 (1993).
[4] *Handbook of Crystal Growth,* edited by D. T. J Hurle (North-Holland, Amsterdam, 1993).
[5] S. Akamatsu and G. Faivre, Phys. Rev. E **61**, 3757 (2000); J. D. Hunt and K. A. Jackson, Trans. Metall. Soc. AIME **846**, 843 (1966).
[6] E. O. Budrene and H. C. Berg, Nature (London) **376**, 49 (1995).
[7] L. Patterson, J. Fluid Mech. **113**, 513–529 (1981).
[8] K. A. Jackson and J. D. Hunt, Acta Metall. **13**, 1212 (1965).
[9] A. M. Turing, Philos. Trans. R. Soc. London B **237**, 37 (1952).
[10] M. Georgelin and M. A. Pocheau, Phys. Rev. E **57**, 3189 (1998).
[11] A. Pocheau and M. Georgelin, J. Cryst. Growth **206**, 215 (1999).
[12] A. Pocheau, V. Croquette, P. Le Gal, and C. Poitou, Europhys. Lett. **8**, 915 (1987).
[13] Y. Kuramoto, *Chemical Oscillations, Waves and Turbulence* (Springer, Berlin, Heidelberg, 1984).
[14] $D(q) = [1 - 3\xi_0^2(q - q_0)^2]/[1 - \xi_0^2(q - q_0)^2]$, ξ_0 denoting a diffusion length and q_0 a wave number in between the cell stability range. Notice that $D''(q)$ is negative.